

Partition, Reaction, and Diffusion Coefficients of Bromine in Elastomeric Polydimethylsiloxane

Maria Eleni Moustaka, Michael M. Norton, Baptiste Blanc, Viktor Horvath, S. Ali Aghvami, and Seth Fraden*



Cite This: *J. Phys. Chem. B* 2021, 125, 5937–5951



Read Online

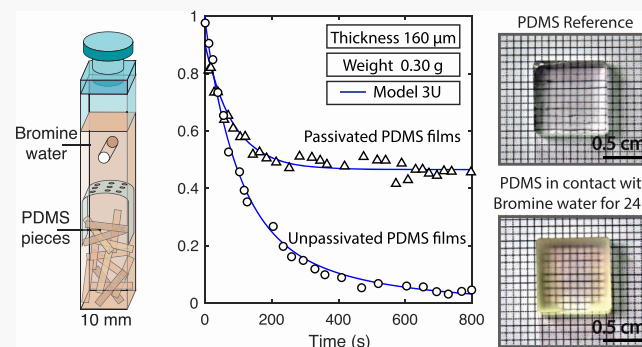
ACCESS |

Metrics & More

Article Recommendations

Supporting Information

ABSTRACT: Experiments and models were used to determine the extent to which aqueous bromine permeated into, and reacted with, the elastomer polydimethylsiloxane (PDMS). Thin films of PDMS were immersed in bromine water, and the absorbance of bromine in the aqueous phase was measured as a function of time. Kinetics were studied as a function of mass and thickness of the immersed PDMS films. We attribute the decrease of bromine in solution to permeation into PDMS, followed by a combination of diffusion, reversible binding, and an irreversible reaction with PDMS. In order to decouple the irreversible reaction from the reversible processes, kinetics were also studied for bromine-passivated PDMS films. Fits of the models to a variety of experiments yielded the partition coefficient of bromine between the water and PDMS phases, the diffusion constant of bromine in PDMS, the irreversible reaction constant between bromine and PDMS, the molar concentration of the reactive sites within PDMS, and the on and off rates of reversible binding of bromine to PDMS. Developing a quantitative reaction–diffusion model accounting for the transport of bromine through PDMS is necessary for the design of microfluidic devices fabricated using PDMS, which are used in experimental studies of the nonlinear dynamics of reaction–diffusion networks containing Belousov–Zhabotinsky chemical oscillators.



INTRODUCTION

Polydimethylsiloxane (PDMS) is one of the most commonly used elastomeric materials in the fabrication of microfluidic devices. Its main advantages are low cost, optical transparency, and ease of processing, such as high-fidelity molding, toughness, and tensile strength. However, PDMS is permeable to liquids with low dielectric constants, which limits its use in microfluidic applications to aqueous solutions.^{1–4} This material is used to fabricate microfluidic devices holding networks of Belousov–Zhabotinsky (BZ) chemical oscillators,^{5–7} where the oscillators in the aqueous compartments (linear dimensions of 30–100 μm) interact via intermediates that diffuse across the PDMS barriers (wall width of 30–100 μm). In a related system, we showed that collective dynamics are governed by the diffusion of the activator, bromous acid (HBrO_2), and bromine (Br_2) which participates in the inhibitory pathway.^{8–12} Due to its low dielectric constant, bromine readily permeates PDMS, separating the BZ compartments, leading to a network of inhibitory coupled chemical oscillators. Bromine plays a key role in the dynamics of the BZ oscillator; therefore, extraneous sources and sinks of bromine alter the oscillatory behavior. PDMS has been used to trigger the nucleation sites of chemical waves¹³ by locally disinhibiting the BZ reaction. Permeation of bromine into PDMS and the reaction of bromine with this could also

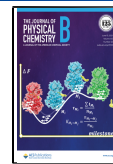
result in the loss of bromine from the BZ compartments, suppressing oscillations if the ratio of the volume of PDMS to the aqueous compartment is large.^{7,14,15} In order to design BZ microfluidic networks in PDMS with predictable properties, the permeation and reaction constants of bromine in PDMS must be known. Developing a quantitative reaction–diffusion model accounting for the transport of bromine through PDMS is the purpose of this work.

Ginn et al. reported the partition coefficient between PDMS and water, $P = [\text{Br}_2]_{\text{PDMS}}/[\text{Br}_2]_{\text{aq}}$, to be 400.¹⁵ Such a high value implies that two adjacent compartments containing BZ should be strongly coupled via the diffusive flux of bromine, which is in disagreement with our previous experimental findings.⁶ The coupling strength between two chemical reactors has been calculated to be proportional to the product of the partition coefficient (P) and the diffusion constant (D) of bromine in the medium separating the reactors.¹² Experiments of BZ reactors

Received: February 19, 2021

Revised: May 13, 2021

Published: May 28, 2021



in PDMS⁷ and finite element models of experiments of BZ chemical waves in PDMS channels⁶ yielded an estimate of $PD = 0.4 \times 10^{-9} \text{ m}^2/\text{s}$.¹² Assessment of the values of P from the measurements of PD requires the independent measurement of D .

However, the diffusion coefficient of bromine in PDMS has not been measured, although the diffusion constant of bromine in octane was measured to be $1.9 \times 10^{-9} \text{ m}^2/\text{s}$.¹⁶ If we assume that the diffusion constant of bromine in PDMS is the same as bromine in octane, then with the estimate of PD from network dynamics we find $P \sim 0.2$. This estimate of the partition coefficient obtained from BZ oscillation dynamics is 3 orders of magnitude smaller than the value obtained spectrophotometrically by Ginn et al.¹⁵ We also note that the measurements of BZ oscillations in octane suggest that $P = 20$, more than an order of magnitude smaller than the value measured for the partition coefficient of bromine in PDMS.¹⁷

Additionally, our recent work with BZ oscillators in PDMS microfluidic devices indicated that bromine reacts with PDMS,⁷ which would have an effect on the previous measurement of the partition coefficient which assumed mass conservation.¹⁵ Other works have shown that PDMS reacts with some chemicals.^{3,18,19} Therefore, it is imperative that the partition constant be re-examined. Here, we report the partition coefficient of bromine between PDMS and water, the diffusion constant of bromine in PDMS, and the extent of reversible and irreversible reactions between bromine and PDMS.

EXPERIMENTAL METHODS

General Description. In order to achieve rapid equilibrium between the aqueous bromine solution and solid PDMS, thin rectangular PDMS films were used. Spectrophotometric determination of bromine inside the PDMS films cannot be carried out directly because the layers are too thin, and PDMS becomes opaque when it is exposed to bromine. Therefore, only the measurement of aqueous bromine was possible in this system (see the schematic representation in Figure 1B). All experiments presented in this work were performed at room temperature (22 °C).

The sample holder consisted of a sealed quartz cuvette containing a thin layer of an inert cyclic olefin copolymer (COC) mesh which separated the cuvette into two parts (Figure 1A). The lower part contained the thin PDMS films to be equilibrated with the bromine solution; the absorbance of the solution was measured in the upper part. The COC mesh contained perforations that allowed for the efficient mixing of the aqueous bromine solution in the cuvette, while preventing any of the films from interfering with the light beam. In order to reach a reduction in bromine concentration that is significant enough to be measured reliably, we needed to place several thin films in contact with the bromine solution. See Section S5 for more details.

Absorption Spectrophotometry. All quantitative measurements were performed using absorbance spectroscopy techniques in the manner as done previously.¹⁵ We submerged thin films of PDMS in an aqueous bromine solution and measured the absorbance as a function of time. We varied the mass and thickness of the PDMS films which were either freshly made or incubated in a solution containing excess of bromine for an extended time in order to eliminate any reactive sites in PDMS.

Throughout the results reported in this paper, initial bromine water concentrations were approximately 12 mM, obtained by

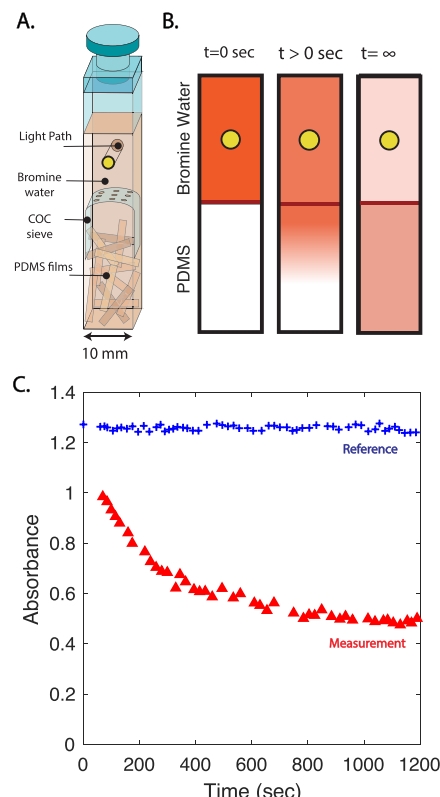


Figure 1. (A) The “measurement” cuvette contains multiple, identical PDMS films immersed in brominated water. A COC sieve prevents PDMS films from obstructing the light path. (B) Schematic representation of the brominated water–PDMS system. Only a single film of PDMS is illustrated for simplicity. Initially, bromine water was placed in contact with a bromine-passivated PDMS elastomer (the red line in the middle is the water–PDMS boundary). Bromine diffuses inside PDMS until the system reaches equilibrium, at which time the bromine concentration is higher in PDMS than in water. The location where light is transmitted through the brominated water is indicated as a yellow dot. (C) Typical raw absorbance data: the blue crosses are the “reference” absorbance data, A_R (brominated water without PDMS). The red triangles are the “measurement” absorbance data A_M (brominated water with PDMS). The measurement and reference cuvettes begin with the same initial concentration of bromine water, 12 mM at a volume of 2.5 mL. The PDMS films are unpassivated in this example with a thickness of 160 μm and total mass of 0.05 g.

mixing $578 \pm 21 \mu\text{L}$ of a saturated bromine water stock solution (0.21 M)²⁰ with 10 mL of deionized water, corresponding to an initial optical density (OD) of 1.4.

We utilized two matching quartz cuvettes with a path length of 10 mm, the first one labeled “reference”, containing a solution of bromine ($[\text{Br}_2]_{\text{aq}} = 12 \text{ mM}$), and the second labeled “measurement,” filled with the same bromine solution as in the reference but in contact with the PDMS films (see Figure 1A). Cuvettes were sealed with glass stoppers and Parafilm; the stock solution was prepared fresh daily. We compensate for the approximately 10% variation in the concentration of aqueous bromine from sample to sample by normalizing absorbances by dividing the “measurement” absorbance by the “reference” absorbance. The measurement and reference cuvettes were filled with the same stock solution at the same time to start the experiment.

The concentration of bromine was determined using Beers law, with the absorbances $A_m = \log(I_m/(I_s)) = elu$ and $A_r =$

$\log(I_r/\langle I_s \rangle) = \epsilon l u_o$, where I_m , I_s , and I_r are the light transmitted through the measurement cuvette (bromine in contact with PDMS), the solvent cuvette (water), and the reference cuvette (identical bromine solution used in the measurement cuvette), respectively. The extinction coefficient of bromine is $\epsilon = 114 \pm 4 \text{ M}^{-1} \text{ cm}^{-1}$ at $\lambda = 404 \text{ nm}$.^{21–23} u denotes the bromine concentration as a function of time, u_o denotes the initial bromine concentration, and $l = 1 \text{ cm}$ is the optical path length. For further details, see Section S4.

The absorbance of bromine in the aqueous phase was measured as a function of time, agitating the measurement cuvette by hand for 5–10 s between time points. Vigorous agitation was necessary to achieve reproducible results. In particular, attention was paid to preventing the thin films from adhering to each other, which limited the transport of bromine from solution to the films. Nearly simultaneous acquisition of absorbance values in the “measurement” and “reference” cuvettes was achieved by taking measurements at each time point consecutively. A typical example of the absorbance data collected during the course of one experiment is shown in Figure 1C. The concentrations of bromine in the two cuvettes are equal initially. The reference absorbance remains nearly constant as a function of time, which indicates that the cuvettes are properly sealed and the interaction of bromine with the COC mesh is negligible. Thus, the large decrease in the absorbance in the measurement cuvette is solely due to the presence of PDMS.

Throughout the paper, we plot experimental results as the normalized absorbance, $A_m/A_r = u/u_o$, the ratio of the absorbance of bromine in contact with PDMS to the absorbance measured in the reference cuvette at the same time point. A_m/A_r is a dimensionless measure of the aqueous bromine concentration as a function of time. In the plots of A_m/A_r , the symbols represent the average, and the error bars indicate the standard deviation resulting from multiple trials of the same experiment. In the plots, only one out of every four data points is plotted for clarity.

PDMS Films. In this study, we used the commercial product Sylgard 184 to produce thin PDMS films. It is supplied as two fluids that were combined at a ratio of 10:1, as recommended by the manufacturer. The components were mixed using a planetary nonvacuum centrifugal mixer (Thinky AR-250) for 6 min. A precisely weighed amount of the mixture was poured onto the center of a 7.62 cm diameter (3 in.) stainless steel wafer, 0.074 cm in thickness, sourced from Stainless Supply. The wafers were then placed in a vacuum chamber and degassed for 3 min, which were then spin-coated using specific spinning programs at room temperature (see Section S2 for program details.) The films were cut into 1.0 cm by 0.2 cm rectangular sections. We chose these dimensions for the length and width of the PDMS films to facilitate loading into the measurement cuvette, to be small enough to move without hindrance while agitating the system between each measurement, and for these two dimensions to be much larger than the remaining dimension so as to validate the approximation that the films can be considered infinite thin planes for which bromine concentration varies only in the direction normal to the plane. The number of 1.0 cm \times 0.2 cm films placed into the measurement cuvette varied with the thickness and total mass of PDMS; see Materials for further details.

Passivated PDMS Films. First, up to 0.3 g of thin PDMS films were added to an Erlenmeyer flask containing 26 mL of 49 mM bromine water. The sealed mixture was kept in the dark

and stirred using a glass magnetic stirring bar for 24 h. The volume of bromine water and the weight of PDMS were chosen, so that the amount of bromine was in great excess over the amount of the reactive sites in PDMS, assuring that no reactive sites remain in PDMS.

Next, the PDMS films were transferred to a Petri dish where they were blotted dry. The films initially appeared opaque, turning from orange to white with time (see Figure 2 and Movie

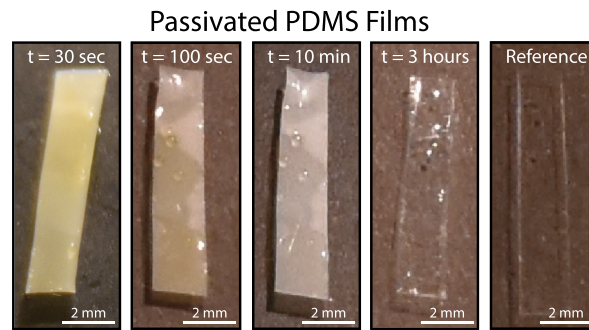


Figure 2. Temporal evolution of PDMS films upon removal from brominated water (26.7 mM). The film was immersed for 46 h. Untreated PDMS is transparent. Treated films are opaque and orange immediately after removal. They lose color in the first few minutes and transform from opaque white to transparent over several hours. For the control, an identical PDMS film was incubated for 46 h in water. This “reference” remained transparent. The thickness of the unpassivated PDMS films is $160 \pm 15 \mu\text{m}$.

S1). The white films were then transferred to 25 mL deionized water in an Erlenmeyer flask and stirred for 5 min. The PDMS films were then transferred to a Petri dish and dried with a tissue.

To verify that the films were bromine-free, they were transferred to a cuvette with 2.5 mL of deionized water, and the absorbance of the aqueous phase was observed 5–10 times while agitating every 5 s. These measurements showed a baseline absorbance at 404 nm for all of the passivated PDMS films.

Lastly, the PDMS films were removed from the cuvette and placed in a Petri dish, blotted dry with a tissue, and allowed to air-dry for another 30 min before use. The passivated films were restored to transparency a few hours after being removed from the bromine water. The elasticity and flexibility of the films remained the same before and after passivation, and there was no measurable change in the thicknesses of the films as a result of the passivation procedure.

■ EXPERIMENTAL RESULTS

Qualitative Observations of PDMS Films Placed in Air, Subsequent to Immersion in Bromine. We undertook a series of qualitative observations to determine whether there were any discernible physical changes to PDMS due to exposure to bromine. We immersed thin PDMS films with a thickness of $160 \pm 15 \mu\text{m}$ in 25 mL of 65 mM bromine water in a sealed Erlenmeyer flask in the dark and mixed using a glass magnetic stirring bar for 24 h. The films were dried with a tissue, placed on a Petri dish, and observed. The opaque films appeared orange and turned to white after 5 min. Subsequently, the transparency of the films was restored after an additional 3 h (see Figure 2 and Movies S1 and S2 in the Supporting Information). The thickness of the films before and after

passivation was identical. We could not measure a difference in the weight of the PDMS films before and after passivation. The PDMS films remained colorless and transparent in the control experiment where the films were placed overnight in deionized water, instead of bromine water.

Time lapse photographs of this process are provided in Figure 2, and videos of the color and transparency changes of the PDMS films are given in the Supporting Information (Movies S1 and S2). These observations suggest that two processes may be present. The initial rapid loss of color could indicate one process, for example, unbound bromine permeating out of PDMS. The slower transformation from white to clear could be due to a different mechanism. Turbidity is caused by heterogeneity in density on the scale of the wavelength of light. One possible explanation for the turbidity is the binding of bromine to PDMS, leading to a microscale collapse of the elastomer. A possible molecular mechanism of the binding is a halogen bond.²⁴ If the halogen bond was reversible, then once the PDMS film was removed from the brominated water, the equilibrium between the bound and unbound bromine would shift, and the bound bromine would unbind and evaporate, causing the PDMS film to revert from opaque white to transparent. The possibility of water permeating into the PDMS film and causing the opacity is excluded by the control, as no change in the transparency of PDMS films was observed when they were immersed in deionized water for 24 h. A similar series of qualitative observations of PDMS cubes of $1\text{ cm} \times 1\text{ cm} \times 1\text{ cm}$ immersed in bromine water and observed as a function of time are shown in the Supporting Information, Section S6. The coloration and opaqueness take a long time to penetrate into the bulk of the PDMS films, as observed by cutting the cubes in half as a function of the duration of bromine exposure.

Ginn et al. pointed out that in a nonacidic bromine solution, besides bromine, a variety of oxybromine species (Br_2 , HOBBr , HBrO_2 , and BrO_3^-) may be present;¹⁵ therefore, they performed their partition measurements in a highly acidic ($[\text{H}_2\text{SO}_4] = 1.0\text{ M}$) bromine solution. To check whether the acidity had any effect on the observed behavior, we performed PDMS passivation using a series of bromine solutions that also contained various amounts of sulfuric acid. The passivated PDMS appeared opaque white at low acidity and nearly transparent when 3.0 M sulfuric acid was present. We note that the acidity of the oscillatory BZ reaction is in the range of 0.3 M $[\text{H}_2\text{SO}_4]$ for which the samples remain highly turbid. Photographs of PDMS immersed in solutions of varying acidity are included in Section S9.

Reaction between Bromine and PDMS. We hypothesize that bromine reacts with some undetermined chemical within PDMS. The total amount of this purported reagent must be small enough to be totally consumed because the bromine absorbance as a function of time saturates at a constant value when the amount of PDMS added to the bromine water is small, as shown in Figure 1C. As the mass of PDMS is increased, the saturation concentration of bromine in solution decreases, and eventually all of the bromine is consumed. If we ignore the accumulation of bromine inside PDMS due to equilibrium partitioning, then we can assume that all bromine that vanishes from the solution has reacted within the PDMS film. For example, in Figure 3A, we observe that all of the bromine initially present in solution vanishes 1000 s after adding 0.30 g of PDMS to 2.5 mL of 12 mM bromine water.

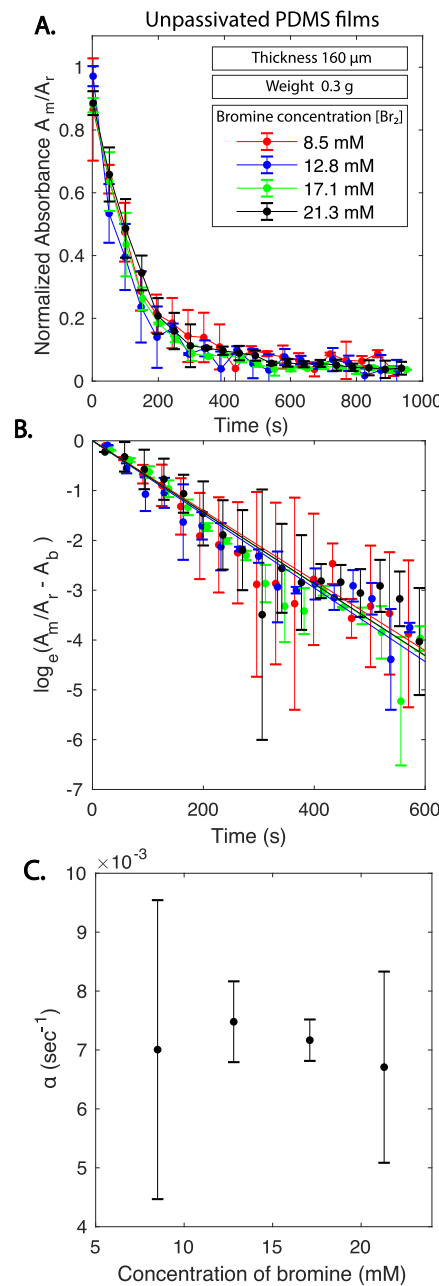


Figure 3. Bromine absorbance as a function of time for unpassivated PDMS films and for different initial concentrations of bromine. The thickness of each PDMS film was $160 \pm 15\text{ }\mu\text{m}$, and the total mass of the films was $0.302 \pm 0.004\text{ g}$. (A) Mean normalized absorbance. There were two samples per bromine concentration, and the error bars represent the standard deviation. For clarity, every fourth data point is plotted. (B) Semi-log plot of the background-subtracted normalized absorbance, $A_m/A_r - A_b$, as a function of time and bromine concentration. All trends are fitted with a line. (C) Decay rates, $\alpha = k[\text{PDMS}]$, are shown as a function of bromine concentration.

We note that the cleavage of the Br_2 bond can release some byproducts in solution, such as Br^- radicals. These will not affect the kinetic analysis made here but could have a significant impact on the behavior of PDMS/BZ networks. Consequently, a better characterization of the post-reacted material and surrounding water solution by methods such as Ag^+ precipitation, MALDI, FESEM, and HPLC would be desirable.

Bromine–PDMS Reaction Order. We hypothesize that bromine reacts with PDMS with the following bimolecular rate equation

$$\frac{d[\text{Br}_2]}{dt} = -k[\text{Br}_2][\text{PDMS}] \quad (1)$$

where k is the reaction constant ($\text{s}^{-1} \text{ mM}^{-1}$), $[\text{Br}_2]$ is the concentration of bromine (mM), and $[\text{PDMS}]$ is the concentration of the bromine reactants in the measurement cuvette (mM). In these experiments, we consider the concentration of PDMS as the total moles of bromine reactants divided by the total volume of the cuvette because we shake the bromine solution and assume that the bromine–PDMS reaction rate is reaction-limited as the PDMS sheets are thin and diffusion is fast. To test this hypothesis, we measured the absorbance of bromine in contact with unpassivated thin PDMS layers. We kept the PDMS mass constant and varied the initial bromine water concentration.

The mass of PDMS was held constant at 0.3 g. This amount of PDMS was chosen so that the number of moles of bromine reactants was large compared to the number of moles of bromine to justify approximating the bromine reactant concentration, $[\text{PDMS}]$, as a constant during the experiments. Figure 3A shows the measured absorbance normalized by the reference absorbance for unpassivated thin PDMS films as a function of bromine concentration and time. All the concentrations have overlapping exponential-like trends. Equation 1 predicts that the normalized concentration is an exponential, $\text{Br}_2(t)/\text{Br}_2(0) = e^{-\alpha t}$, with $\alpha = k[\text{PDMS}]$, a constant that depends on the concentration of PDMS. A semi-log plot of the background-subtracted normalized absorbance, $A_m/A_r - A_b$, is shown in Figure 3B. The background, A_b , was determined from the mean of the last 10 absorbance values. The data support the hypothesis as this plot is linear with a regression coefficient of $R^2 = 0.90$. Figure 3C shows the decay rate as a function of bromine concentration. The decay rate is a constant, $\alpha = 7 \times 10^{-3} \text{ s}^{-1}$, independent of bromine concentration, as expected when the reaction is first-order in bromine concentration. This result is qualitatively consistent with the presence of a reaction between bromine and PDMS determined from modeling the period of the BZ oscillation as a function of PDMS mass.

Passivated PDMS. In order to separate the dynamics of diffusion from that of reaction, experiments were performed on passivated PDMS samples, as described in **Passivated PDMS Films**, which were prepared through immersion for a long time in excess bromine to assure that all the bromine reactants in PDMS were consumed.

We performed two sets of absorbance experiments to study the interaction of bromine and passivated PDMS.

Passivated PDMS Films with Same Thickness and Different Masses. In the first set of absorbance experiments, the thickness of the PDMS films was held constant at $h = 160 \pm 15 \mu\text{m}$, and the total mass of the PDMS films in the cuvette was varied. Four different PDMS masses were studied, and each experiment was performed twice (see *Section S7*). In Figure 4 we show the normalized absorbance as a function of time for two masses of passivated films of thickness $h = 160 \mu\text{m}$. Two of the four masses were plotted for increased clarity.

Passivated PDMS Films with Same Mass and Different Thicknesses. In the second set of absorbance experiments, the mass of the films was held constant at $m = 0.15 \text{ g}$, and the thickness of the PDMS films was varied. In Figure 5 we show

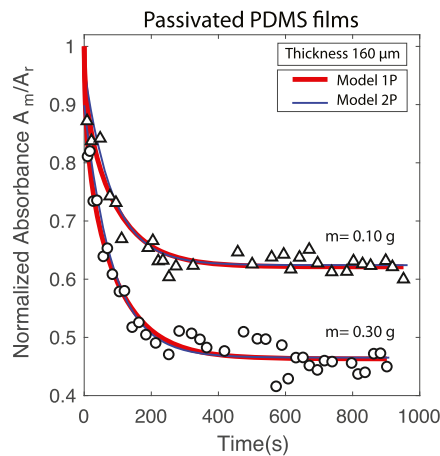


Figure 4. Normalized bromine absorbance as a function of time for passivated PDMS films at constant thickness ($160 \pm 15 \mu\text{m}$) and different masses. Data: triangles (0.10 g of PDMS) and circles (0.30 g of PDMS). Fit models are described in **Theoretical Methods**: red line (Model 1P), blue line (Model 2P).

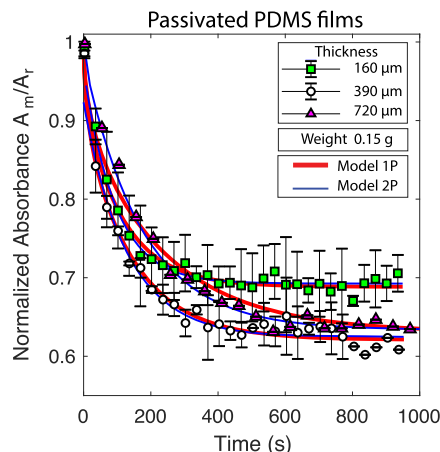


Figure 5. Normalized bromine absorbance as a function of time for passivated PDMS films at constant mass (0.15 g) and different thicknesses; 160, 390, and $720 \mu\text{m}$. The initial concentration of bromine $[\text{Br}_2]$ was $\sim 12 \text{ mM}$ for all samples. The fit models are described in **Theoretical Methods**: red line (Model 1P), blue line (Model 2P). Every fourth data point is plotted. The data shown are the average of two samples for each PDMS thickness.

the normalized absorbance as a function of time for films of the same mass but of different thicknesses. If the time dependence of the absorbance was diffusion-limited, then the time for the absorbance to decay would scale as the square of the thickness. However, no significant difference in either the time for the absorbance to decay or the saturation value is observed in Figure 5. As the films are passivated, there is no irreversible reaction, but there can still be reversible reactions. The fact that the time dependence is independent of thickness implies that reversible binding is the rate-limiting step.

Unpassivated PDMS Films with Same Thickness and Different Masses. In Figure 6 we present bromine absorbance measurements on unpassivated PDMS films with a constant thickness, $160 \pm 15 \mu\text{m}$, as a function of PDMS mass and time. The bromine concentration decreases and plateaus at a steady value that decreases with increasing PDMS mass. We hypothesize that bromine reacts with some undetermined chemical within PDMS. The total amount of this purported

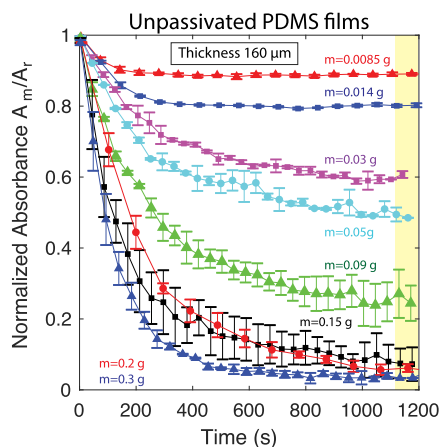


Figure 6. Normalized absorbance ($A = A_m/A_r$) of thin, unpassivated PDMS films of constant thickness ($160 \pm 15 \mu\text{m}$), as a function of mass and time. The initial concentration of bromine $[\text{Br}_2]$ was 12 mM. Every fourth data point is plotted. The data shown are the average of either two or three samples for each PDMS mass, 19 trials in total.

reagent must be small enough to be totally consumed because the bromine absorbance as a function of time saturates at a constant value when the amount of PDMS added to the bromine water is small, as shown in Figure 6. As the mass of PDMS is increased, the saturation concentration of bromine in solution decreases, and eventually all of the bromine is consumed. If we ignore the accumulation of bromine inside PDMS due to equilibrium partitioning, then we can assume that all bromine that vanishes from solution has reacted within PDMS. For example, in Figure 6, we observe that all of the bromine initially present in solution vanishes 1200 s after adding 0.15 g of PDMS to 2.5 mL of 12 mM bromine water. The molecular weight of the monomer of PDMS, dimethyl siloxane (DMS), is 75 g/mol; so, initially, the cuvette contained 3×10^{-5} mol of Br_2 and 2×10^{-3} mol of DMS. If we assume that all of the bromine reacted with DMS, then about 1% of the DMS molecules are reactive with bromine, or the number of moles of the bromine reactant is 3×10^{-5} mol. The lack of stoichiometry between the bromine reactant and DMS suggests that bromine does not react with DMS. As the density of PDMS with a 1:10 cross-link density is $\rho = 1.07 \text{ g/mL}$ ²⁵ (see Section S3), the volume of 0.15 g of PDMS is $1.4 \times 10^{-4} \text{ L}$, and therefore the molar concentration of the bromine reactant in PDMS, which we refer to as w_o , is $w_o = 244 \text{ mM}$ (see Section S8).

Unpassivated PDMS Films with Same Mass and Different Thicknesses. Here, we present absorbance measurements on unpassivated PDMS films with constant mass as a function of PDMS thickness and time. We observed that the decay rates of the absorbance of unpassivated PDMS films with thicknesses lower than $160 \mu\text{m}$ are independent of thickness. The implication is that diffusion is fast for films smaller than $160 \mu\text{m}$ and that the process is reaction-dominated. Figure 7 shows the absorbance versus time for unpassivated PDMS films with constant mass, 0.1 g, and for four different thicknesses, 160, 320, 480, and $720 \mu\text{m}$. The rate of bromine absorbance varies with thickness for layers thicker than $300 \mu\text{m}$, which implies that for these thicknesses, both diffusion and reaction are important.

Nature of Reactants. It has been reported that a low concentration of uncross-linked low-molecular weight

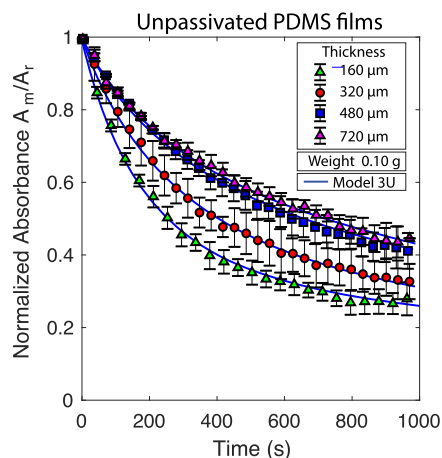


Figure 7. Normalized absorbance of unpassivated PDMS films as a function of thickness and time. All samples weigh 0.1 g. Thickness: 160 μm (green triangles), 320 μm (red circles), 480 μm (blue squares), and 720 μm (magenta triangles). The fit model is described in the Results and Discussion: Blue line (Model 3U). Every fourth data point is shown for clarity. The data shown are the average of two samples for each PDMS thickness.

oligomers remains after cross-linking for Sylgard 184, the silicone elastomer PDMS used in this study.^{26,27} To evaluate the potential of these uncross-linked PDMS contaminants as possible reactants with bromine, we followed an extraction method published by Lee et al.²⁶ Fresh PDMS were swelled in either 10 mL or 20 mL of xylene for 24 h while stirring constantly. Then, the films were removed from xylene and baked at 70 °C for 24 h. The weight of each of the samples before the xylene treatment was about 0.3 g, and the weight loss of PDMS after xylene treatment was about 5% for all treated samples. This loss agrees with the findings of Lee et al.,²⁶ indicating that the extraction treatment was successful. No significant difference between the absorbance measurements of the treated and untreated films as a function of time was observed (see Figure 8). As the extraction treatment did not decrease the reactivity, this result indicates that the bromine-reactive sites are bound to the solid PDMS and that the mobile uncross-linked components are not the source of the irreversible chemical reaction between Sylgard 184 and bromine.

Partition Coefficient. The partition coefficient is defined as the ratio of the equilibrium concentrations of a substance dissolved in each of two materials, between which the substance freely exchanges. Specifically, we are interested in the partition coefficient of bromine between PDMS and water, defined as

$$P = \frac{[\text{Br}_2]_{\text{PDMS}}}{[\text{Br}_2]} \quad (2)$$

We estimated the partition coefficient by using the absorbance data collected from the aqueous phase of the measurement cuvette (see Section S5, Figure 2) to determine the concentration of bromine in water, $[\text{Br}_2]$. The concentration of bromine in PDMS, $[\text{Br}_2]_{\text{PDMS}}$, can be deduced by assuming mass conservation, for example, bromine removed from water has passed to PDMS. With these assumptions, we obtain the following formula for the partition coefficient

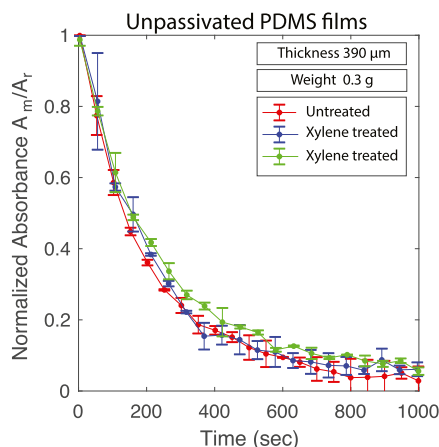


Figure 8. Extraction of uncross-linked PDMS contaminants. The mean absorbance of bromine in the presence of PDMS films as a function of time before and after xylene treatment. The data shown are the average of two samples for each case. The red curve is the untreated film. The green and blue curves correspond to the two different xylene extraction treatments described in the text. The unpassivated films had a thickness of $390 \pm 20 \mu\text{m}$ and weighed 0.3 g. The initial concentration of bromine was 12 mM. Every fourth data point is plotted.

$$P = \frac{V_{\text{aq}}}{V_{\text{p}}} \left[\frac{A_{\text{Br}_2 \text{ initial}}}{A_{\text{Br}_2 \text{ final}}} - 1 \right] \quad (3)$$

where V_{aq} and V_{p} are the volumes of water and PDMS in the measurement cuvette, respectively; $A_{\text{Br}_2 \text{ final}}$ is the absorbance of bromine in the reference cuvette; and $A_{\text{Br}_2 \text{ final}}$ is the absorbance of bromine in the measurement cuvette containing well-mixed bromine and PDMS films at a time long enough such that the bromine concentrations in the water and PDMS phases have equilibrated. The same formula and experimental method were used previously by Ginn et al.¹⁵ In Figure 1C, the absorbance at large times is constant, indicating equilibrium between the bromine concentration in water and PDMS. We consider this time-independent value of the absorbance as $A_{\text{Br}_2 \text{ water final}}$. Figure 6 presents the normalized absorbance measurements of thin, freshly made unpassivated PDMS films of the same thickness, $h = 160 \mu\text{m}$, as a function of the mass of the films. Here, and in the remainder of the paper, we present the normalized absorbance as $A = A_m/A_r$, where A_r is the mean absorbance value of the reference and is the same concentration as the initial bromine concentration in the cuvette with PDMS.

In Figure 6, we observe that the bromine concentration in water in contact with PDMS decreases with time, and the rate of decrease in concentration increases with the PDMS mass. We calculate the bromine PDMS/water partition coefficient by assuming that all the missing bromine partitions into PDMS and ignore any loss due to reaction. An upper bound on the partition coefficient is found by considering the absorbance value measured at 1200 s in Figure 6 as the equilibrium value. If these assumptions are correct, then the partition coefficient should be a constant, independent of the mass of PDMS, as shown in Figure 9. As we performed our experiments in the same manner as Ginn et al. who measured the partition coefficient $P = 400$ for one mass of PDMS, we expected to obtain this same value of P for all PDMS masses.¹⁵ The fact that the calculated partition coefficient is not constant indicates that the assumption that bromine mass is conserved is wrong, and the fact that the calculated partition coefficient increases

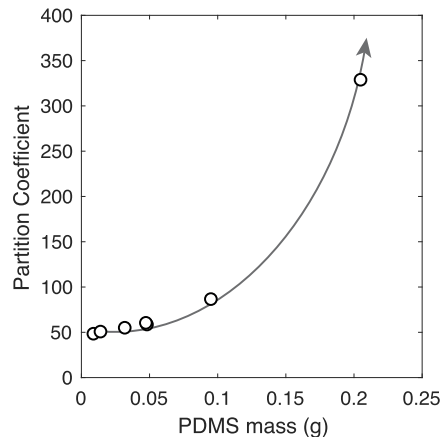


Figure 9. Bromine partition coefficient measured from unpassivated PDMS films calculated using eq 3, with the mean absorbance taken at $t = 1200$ s (Figure 6). The partition constant is not constant.

monotonically as a function of PDMS mass implies that more bromine has disappeared than can be accounted for via partitioning alone. An explanation is that some of the bromine species irreversibly reacted with a compound within PDMS, which is consistent with our estimation that PDMS contains bromine reactants at a concentration of ~ 240 mM.

Role of Acidity in Bromine/PDMS Reaction–Diffusion.

The motivation for this work was to assess the degree to which bromine interacts with PDMS. Ginn et al. raised the point that acidity alters the bromine species in water and suggested that this could have an impact on the reaction of bromine with PDMS.¹⁵ To assess this possibility, we performed a few absorbance experiments with passivated and unpassivated films in the conditions identical to a typical BZ reaction (80 mM H_2SO_4 and 288 mM NaBrO_3) and found no differences in the absorbance, indicating that for BZ conditions, acidity plays no role in the transport of bromine through PDMS. However, at higher acidity values (3 M sulfuric acid), we observed that PDMS in brominated water became transparent. (See Section S9 for more details). One caveat is that Ginn et al. performed their measurements at 1 M H_2SO_4 to prevent the formation of other bromine species, while we performed our measurements in water¹⁵ and in the solutions of the BZ reaction. It is possible that one of the bromine species that forms in pure water reacts with PDMS but does not form in 1 M sulfuric acid, accounting for the differences between the results of Ginn et al.¹⁵ and ours.

THEORETICAL METHODS

Three Models. We considered three models to describe the absorbance measurements of bromine in water in contact with the thin films of PDMS. In Model 1P, we considered bromine to permeate into passivated PDMS where it freely diffuses. This model has two fitting parameters: the partition constant (P_1) and the diffusion constant of bromine in PDMS (D_u). Model 1P is designed to account for the first process described in Qualitative Observations of PDMS Films Placed in Air Subsequent to Immersion in Bromine: the rapid loss of the orange color of PDMS films after removal from brominated water, which we ascribe to the permeation and diffusion of bromine in PDMS.

In Model 2P, we again considered passivated PDMS in which reversible bromine–PDMS binding occurs throughout the PDMS interior, introducing additional on (k_+) and off (k_-) rate

constants as fitting parameters and ignoring diffusion. Model 2P is designed to account for the second process described in **Qualitative Observations of PDMS Films Placed in Air Subsequent to Immersion in Bromine**: the transition from turbidity to transparency of PDMS films after they are removed from brominated water, which we ascribe to the reversible binding of bromine to PDMS, perhaps in the form of a halogen bond. The second motivation underpinning Model 2P is that the rate of absorbance was independent of the PDMS film thickness (Figure 5), indicating that diffusion was not a factor in the absorbance rate. In Model 2P, we restrict ourselves to thin films wherein diffusion is fast compared to the reversible binding/unbinding kinetics. In this limit, diffusion can be ignored, and the concentration of bromine in PDMS is considered to be spatially uniform at all times. Formally, this model assumes that the Damköhler number, defined as the ratio of diffusive and reaction timescales, $Da = \tau_D/\tau_k \ll 1$. We will validate this assumption after identifying all parameters.

Model 3U considers bromine in unpassivated PDMS films. It is the most general model, combining the elements from Model 1P and Model 2P and adding additional ones. In Model 3U, bromine permeates into PDMS, freely diffuses as well as reversibly binds to PDMS, and additionally irreversibly reacts with a fixed number of bromine reactants on PDMS with a concentration (w_0) characterized by the reaction rate between the bromine reactant and bromine (k_{uw}). With generality comes the price of extra fitting parameters. The hope is that some of the fitting parameters in Model 3U could be fixed by first doing experiments on passivated films and analyzed with Models 1P and 2P.

In all models, we considered PDMS to be a film that is much thinner in one dimension than the other two. The disparity between these length scales allows us to ignore mass transport through all but the largest faces, thereby reducing the mass transport model within PDMS to a single spatial dimension such that $\partial_x \neq 0$ and $\partial_y, \partial_z = 0$. In the experiment, we employed multiple, identical thin films in which the thin direction is much smaller than the other two directions, satisfying the assumptions of our model. We established a coordinate system, shown in Figure 10, in which the boundary between the bromine water and PDMS is located at $x = 0$ (dark red line). The concentration of dissolved bromine in water, $u_\infty(t)$, located throughout the region $x < 0$ is considered spatially uniform because the solution is shaken frequently. In Models 1P and 3U, the bromine concentration to the right side of the boundary, $x > 0$, varies in space and time due to the combined actions of reaction and diffusion. At the interface $x = 0$, different conditions for each model link the domains and are given below. The concentration u_∞ evolves according to the mass conservation equation

$$\frac{du_\infty}{dt} = \mu \frac{\partial u}{\partial x} \Big|_{x=0}, \quad t > 0 \quad (4)$$

where $u(x, t)$ is the unbound, mobile bromine concentration within PDMS, and $\mu = D_u A/V$ is the diffusive mass transfer rate defined in terms of the total contact area between PDMS and water A , the volume of the aqueous phase V , the bromine diffusion constant within PDMS, D_u and the concentration gradient of bromine within PDMS. We calculated the contact area as $A = 2V_p/L$, with L being the thickness of the PDMS films and V_p the total volume of PDMS, thereby neglecting the contributions from the edges of the thin PDMS films. This

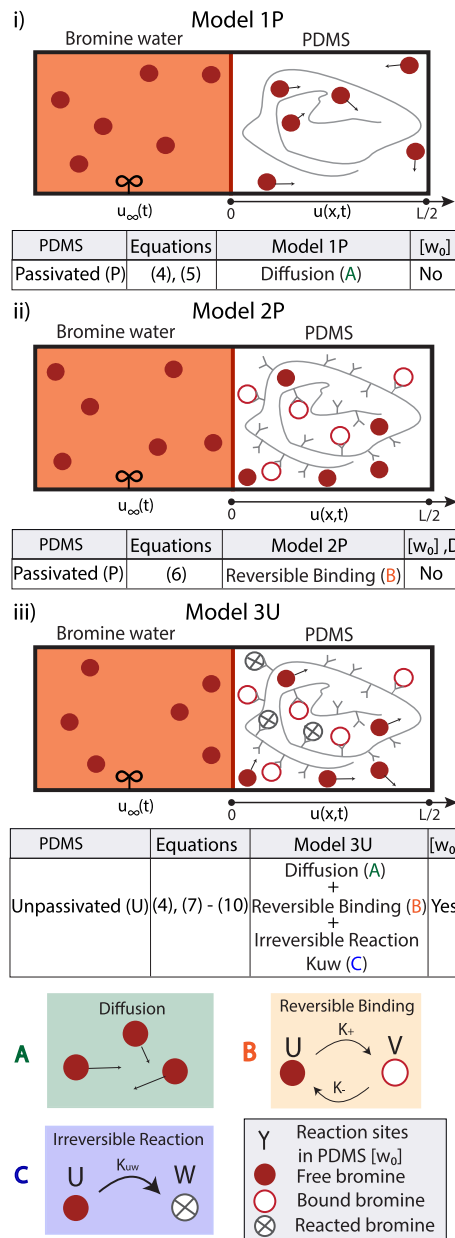


Figure 10. Schematic representation of the computational fitting models: (i) Model 1P: mobile bromine (red disks, u) is well mixed by agitation in the aqueous phase (left side). Bromine freely diffuses in the passivated PDMS polymer (right side). (ii) Model 2P: mobile bromine diffuses rapidly and reversibly binds (red circles, v) to the passivated PDMS polymer with on (k_+) and off (k_-) rates. (iii) Model 3U: mobile bromine diffuses in unpassivated PDMS as in Model 1P, reversibly binds to PDMS as in Model 2P, and irreversibly binds with the reactants ("Y" symbol, w_0) with reaction rate k_{uw} .

model assumes that PDMS is not porous, which is supported by positron lifetime measurements that indicate the average pore diameter in PDMS is less than a nanometer.²⁸

Model 1P: Passivated PDMS, Partition, and Diffusion. In order to separate the dynamics of diffusion from that of reaction, we considered passivated PDMS samples, in which all the bromine reactants in the PDMS film were consumed through exposure to excess amounts of bromine. The instantaneous gradient $\frac{\partial u}{\partial x} \Big|_{x=0}$ is found by simultaneously solving the diffusion equation

$$\frac{\partial u}{\partial t} = D_u \frac{\partial^2 u}{\partial x^2}, \quad x \in (0, L/2] \quad (5)$$

with the bulk dynamics of eq 4. The bromine concentrations on each side of the boundary between the aqueous PDMS phases are related by the partition coefficient P_1 such that $u(x=0, t) = P_1 u_\infty(t)$ for $t > 0$. This matching condition, along with the no-flux boundary condition at the other end of the region $\frac{\partial u}{\partial x} \Big|_{x=L/2} = 0$, provides the necessary boundary conditions for u .

The initial concentration of bromine in solution, $u_\infty(t=0) = u_{\infty,0}$, is controlled experimentally. We assumed that PDMS is initially devoid of bromine, $u(x > 0, t=0) = 0$.

Model 2P: Passivated PDMS, Partition, and Reversible Reaction. In Model 2P, we consider reversible binding to PDMS, $u \xrightleftharpoons[k_-]{k_+} v$, with $v(x,t)$ being the concentration of bound bromine. This reversible reaction introduces two new rate constants, k_+ and k_- . Model 2P ignores irreversible reactions and thus is only applicable to passivated films. Furthermore, Model 2P assumes that diffusion is fast compared to binding/unbinding kinetics. This separation of timescales eliminates the spatial derivatives of u and, consequently, the concentration of unbound bromine u inside PDMS is now assumed to always be identical to that of the bromine concentration in the aqueous solution, u_∞ . We therefore let $u(t)$ represent the PDMS–water system's bromine concentration. The dynamics of u can then be given by the following first-order, lumped parameter model

$$\begin{aligned} \frac{du}{dt} &= \phi(k_- v - k_+ u), \\ \frac{dv}{dt} &= (k_+ u - k_- v) \end{aligned} \quad (6)$$

where $\phi = V_p/(V_{\text{aq}} + V_p)$ is the volume fraction of PDMS, V_p is the volume of PDMS, and V_{aq} is the volume of water. The on/off rates for the reversible binding of bromine, k_\pm , are related through a new partition coefficient, $P_2 = k_+/k_-$. Model 2P considers PDMS to contain two species of bromine, one bound (v) and the other unbound (u). Consequently, the effective partition coefficient of the entire solid is $P_2^* = P_2 + 1$. It is P_2^* of Model 2P that should be compared with P_1 of Model 1P.

We assume that no bromine is bound to the solid initially, $v(t=0) = 0$. However, the initial condition for the unbound bromine is adjusted to account for the dilution that occurs when bromine first permeates the PDMS film via rapid diffusion but before any binding takes place. In order for mass conservation to be preserved in Model 2P, we must alter the initial condition such that $u(t=0) = (1 - \phi)u_{\infty,0}$.

Model 3U: Unpassivated PDMS, Partition, Diffusion, and Reversible and Irreversible Reactions. In Model 3U, we combine the diffusion dynamics of eqs 4 and 5 with the reversible binding of bromine to PDMS, $u \xrightleftharpoons[k_-]{k_+} v$, eq 6, and an additional, irreversible reaction k_{uw} between bromine $u(x,t)$ and the reactants located on the PDMS polymer $w(x,t)$ to give

$$\frac{\partial u}{\partial t} = D_u \frac{\partial^2 u}{\partial x^2} - k_{uw} u w - k_+ u + k_- v \quad (7)$$

$$\frac{\partial v}{\partial t} = k_+ u - k_- v \quad (8)$$

$$\frac{\partial w}{\partial t} = -k_{uw} u w \quad (9)$$

Like Model 2P, the effective partition coefficient of the entire solid is $P_2^* = P_2 + 1$. It is P_2^* of Model 3U that should be compared with P_1 of Model 1P. We assume that both forms of bromine are absent from the solid initially, $v(x, t=0) = 0$ and $u(x, t=0) = 0$, and that the PDMS reactants are uniformly distributed initially, $w(x, t=0) = w_0$. In Section S10, we show that Model 3U limits to the form of Model 1P when $k_{uw} = 0$, and reversible kinetics are fast but with a new effective diffusion coefficient that depends on the partition coefficient.

Numerical Methods. Models 1P and 3U were solved using the method of lines: the Laplacian operator was discretized using 200 grid points over the half domain, $[0, L/2]$, to produce a system of ODEs that was then integrated in Matlab. Model 2P, eq 6, was solved analytically. See Section S10 for more details.

RESULTS AND DISCUSSION

The models we use to describe the temporal behavior of bromine in water in contact with PDMS involve up to six fitting parameters in the case of Model 3U. These are too many to fit reliably and uniquely, given the level of experimental noise and the structure of the models. Therefore, our strategy is to first analyze bromine absorbance experiments on passivated PDMS because passivation eliminates w_0 and k_{uw} as fitting parameters. The procedure is to establish some of the fitting parameters through experiments on passivated PDMS and then treat these parameters as constants when analyzing the experiments performed on unpassivated films. There are three unknown parameters for Model 1P, $\{D_u, P_1, t_{\text{shift}}\}$, and for Model 2P, $\{P_2 = k^+/k_-, k^+ \text{ or } k_-, t_{\text{shift}}\}$, while for Model 3U, there are six unknown parameters, $\{D_u, P_2 = k^+/k_-, k^+ \text{ or } k_-, k_{uw}, w_0, t_{\text{shift}}\}$. In all these cases, the parameters are found by minimizing the sum of the squared errors between the experimental observations of the concentration of bromine in the water phase and the model prediction $E = \sum_{i=1}^N [u_{\infty, \text{exp}}(t_i) - u_{\infty, \text{th}}(t_i)]^2$. The parameter t_{shift} accounts for the uncertainty at the start time of the experiment. The parameter fits were performed on each measurement of A_m/A_r and then the results were averaged together and standard errors were calculated.

Fits: Passivated PDMS Films with Constant Thickness and Different Masses. Model 1P and Model 2P are used to fit the absorbance measurements from passivated PDMS samples with constant thickness and four different masses, as shown in Figure 4. Two data sets were recorded and analyzed per PDMS mass (eight measurements in total). Model 1P treats the transient dynamics as arising from the free diffusion of bromine in PDMS, while Model 2P considers the dynamics to arise from the reversible binding of bromine to PDMS. Representative samples of the model fits and experimental data are shown in Figure 4, where the fits to Model 1P are shown with a red line and those to Model 2P with blue lines. Table 1 lists the fitting parameters for Models 1P and 2P.

Model 2P yields the on and off rates, plotted as a function of PDMS mass in Figure 11A,B. The partition coefficients for both Model 1P and Model 2P are plotted in Figure 11C, and the diffusion coefficient for Model 1P is plotted in Figure 11D. The fits systematically decrease as the PDMS mass increases, while theory considers the parameters to be independent of the PDMS mass. Such systematic variations of the fits indicate a

Table 1. Model Parameters for Passivated PDMS Films^a

parameters	Model 1P	Model 2P	physical meaning
P_1	fit	1	partitioning at the PDMS–water boundary
k_-	n/a	fit	conversion rate, vu (reversible)
k_+	n/a	fit	conversion rate, uv (reversible)
D_u	fit	∞	diffusivity of bromine in PDMS
k_{uw}	0	0	reaction between unbound bromine and PDMS
w_o	0	0	concentration of bromine reaction sites on PDMS
t_{shift}	fit	fit	time shift applied to experimental data

^aFixed parameters are listed as numbers, those varied are designated by “fit”, and those absent in a model by “n/a”. The assumption is that passivated PDMS and bromine do not react; hence, $k_{uw} = w_o = 0$.

shortcoming in the model or a systematic error in the experiment. A summary of the average fitted values of the partition constant (P), diffusion (D) constant, and the on (k_+) and off (k_-) rates for the passivated thin PDMS films is given in Table 2.

Fits: Passivated PDMS Films with Constant Mass and Different Thicknesses. We performed experiments on passivated PDMS films with the same mass ($m = 0.15$ g) for three different thicknesses: 160 μm (two data sets), 390 μm (two data sets), and 720 μm (one data set). Figure 5 shows the average absorbance for each thickness as a function of time

Table 2. Summary of Fitting Results for Passivated PDMS Films with Constant Thickness ($h = 160 \mu\text{m}$) and Different Masses^a

coefficients	Model 1P	Model 2P
$k_- (\text{s}^{-1})$	n/a	0.0062 ± 0.0024
$k_+ (\text{s}^{-1})$	n/a	0.071 ± 0.033
P_1, P_2^*	12 ± 3	12 ± 3
$D_u (10^{-9} \text{ m}^2/\text{s})$	0.019 ± 0.0067	∞

^aThe absorbance measurements are shown in Figure 4.

along with the fits of Model 1P (red line) and Model 2P (blue line). No significant difference in absorbance is observed as a function of thickness for the passivated PDMS films of the same total mass (Figure 5). As the films are passivated, there can be no irreversible reaction, but there can still be reversible reactions. If the time dependence of the absorbance was due to bromine diffusion, then the decay time would vary with the square of the thickness. The implication is that the absorbance of the 720 μm film should decrease 16 times slower than the absorbance of the 160 μm film. The fact that the time dependence is independent of thickness invalidates diffusion as an explanation of the time dependence. We instead hypothesize that reversible binding is the rate-limiting step. Equivalently, we conclude that the ratio of diffusive and reaction timescales given by the Damöhler number for these experiments must be of

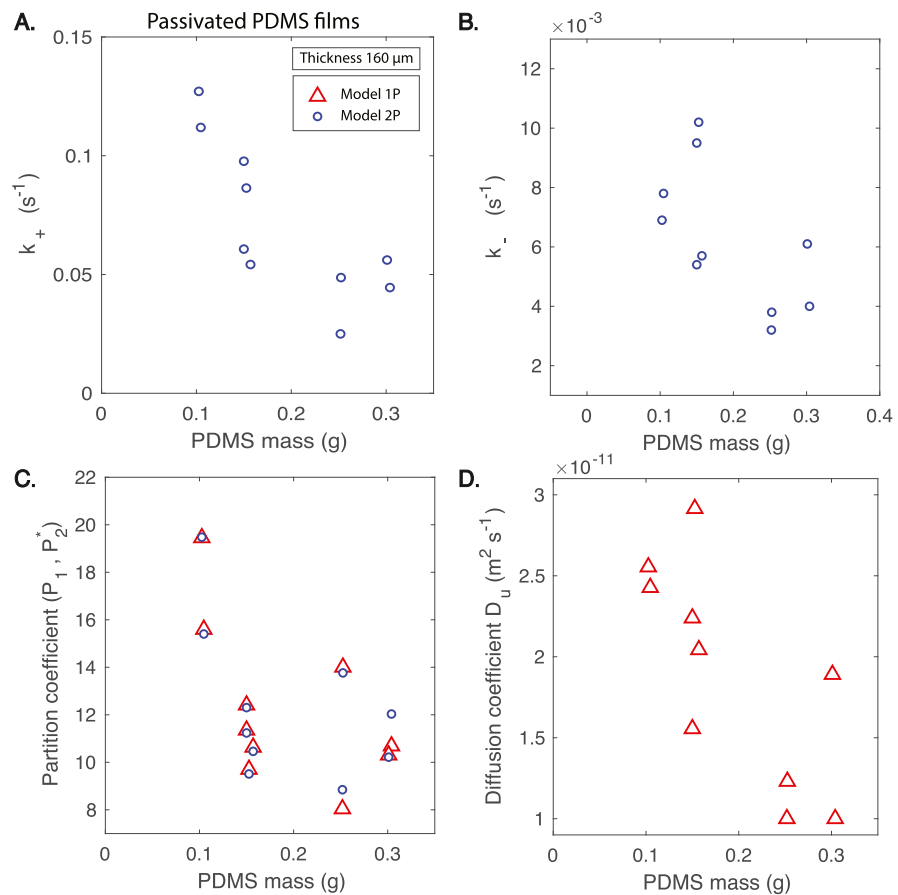


Figure 11. Fitting results for Model 1P (red triangles) and Model 2P (blue circles) from the absorbance measurements (Figure 4) of passivated PDMS films with constant thickness (160 μm) and different masses. The average values are listed in Table 2. (A) On rate (k_+). (B) Off rate (k_-). (C) Bromine partition coefficients P_1 and P_2^* . (D) Diffusion coefficient, D_u .

order 1 or less. We define Da for the reversible reactions in Model 2P/3U as

$$Da = \frac{\tau_D}{\tau_k} = \frac{k_+(L/2)^2}{D_u} \quad (10)$$

The fitting coefficients obtained with the use of Model 1P and of Model 2P are shown in Table 3. P_1 and P_2^* , which are the

Table 3. Summary of Fitting Results for Model 1P and Model 2P^a

coefficients	$h_1 = 160 \mu\text{m}$	$h_2 = 390 \mu\text{m}$	$h_3 = 720 \mu\text{m}$
Model 1P			
P_1	12	12	12
$D_u (10^{-9} \text{ m}^2/\text{s})$	0.019	0.097	0.18
Model 2P			
$k_- (\text{s}^{-1})$	0.0075	0.0060	0.0036
$k_+ (\text{s}^{-1})$	0.079	0.064	0.040
P_2^*	12	12	12

^aPassivated PDMS films with constant mass ($m = 0.15 \text{ g}$) and different thicknesses. The absorbance data are as in Figure 5.

partition constants for bromine between water and PDMS for Models 1P and 2P, respectively, do not vary with thickness and are equal. The fact that the result is the same for different models and for different thicknesses gives us high confidence in this value of the partition constant.

In the fits to Model 1P, the diffusion coefficient, D_w increases by a factor of 10 as the passivated film thickness increases by a factor of 4 (Table 3). The inability of Model 1P to fit the data from the passivated films of different thicknesses with the same diffusion constant indicates that the assumptions of the model are wrong. Therefore, we do not use values for D_w obtained from Model 1P for further analysis in Model 3U. Model 2P fared better. The on and off rates produced by Model 2P only vary by a factor of 2 as the thickness increases by a factor of 4 (Table 3). Variation by a factor of 2 in the on and off rates is a significant systematic variation of the fitting constants but is a much smaller variation than the factor of 10 returned by Model 1P for the diffusion constant. Note that Model 1P ignores the reversible binding of bromine to PDMS, while Model 2P treats the free diffusion of bromine inside PDMS to be so rapid that the bromine concentration is always uniform. The truth may be that these experiments (Figure 5) are not completely in the reaction-limited regime and that both the reversible reaction and diffusion contribute to the absorbance kinetics. Our results show that we are unable to disentangle them; so, for simplicity, we assume reaction-limited dynamics while acknowledging that they may be contaminated by diffusive effects.

Fits: Unpassivated PDMS Films with the Same Thickness and Different Masses. Here, we fit the absorbance data shown in Figure 6 to Model 3U. As indicated in Table 4 we fix the on (k_+) and off (k_-) rates and partition coefficient (P_2^*) using the values obtained from fits to data on passivated films (Table 3). Our prior estimate of the bromine reactant concentration, $w_o = 244 \text{ mM}$, is used to constrain w_o in the fits to a range of possible values, $0 < w_o < 400 \text{ mM}$. The fitting parameters for Model 3U are D_w , k_{uw} , and w_o (Table 4). Representative examples of the normalized absorbance data and fits to Model 3U for two different masses of unpassivated PDMS are shown in Figure 12. Model 3U provides a good fit of the data with masses higher than 0.03 g, and fits for experiments

Table 4. Fitting Parameters for Model 3U for Unpassivated PDMS Films^a

parameters	Model 3U
P_2^*	12
$k_+ (\text{s}^{-1})$	0.071
$k_- (\text{s}^{-1})$	0.0062
$D_u (10^{-9} \text{ m}^2/\text{s})$	fit
k_{uw}	fit
$w_o (\text{mM})$	fit [0–400]
t_{shift}	fit

^aThe parameters that are varied are designated by “fit”. Model 3U has six fitting parameters in general, but two were set by measurements on passivated films (Table 2). Not all the parameters are independent as $P_2^* = k_+/k_-$. Model 3U accounts for the reversible binding of bromine to PDMS, free diffusion of bromine in PDMS, and irreversible reaction between free bromine and PDMS.

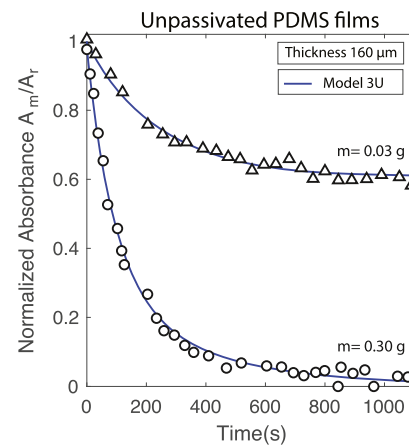


Figure 12. Normalized bromine absorbance vs time for unpassivated PDMS films of thickness $160 \pm 15 \mu\text{m}$. Data: triangles (0.03 g PDMS) and circles (0.3 g PDMS). Fits: blue line, Model 3U, described in the Theoretical Methods section. The data shown in this figure are the same as in Figure 6. The fitting results are summarized in Table 5.

with masses lower than 0.03 g were not included in the analysis because the fits were poor.

Fits as a function of PDMS mass of the reaction constant (k_{uw}), the concentration of reactants (w_o), and the diffusion constant (D_u) are shown in Figure 13A–C. The averaged values of these three fitting coefficients are summarized in Table 5. The reaction constant between bromine and the bromine reactants in PDMS is found to be $k_{uw} = 6.77 \times 10^{-4} \text{ s}^{-1} \text{ mM}^{-1}$. The concentration of the reactants is $w_o = 270 \text{ mM}$, which is very close to the value of 244 mM that we estimated and applied as an initial value during fitting (see Supporting Information). The diffusion constant is $D_u = 0.38 \times 10^{-9} \text{ m}^2/\text{s}$.

The reaction rate for the consumption of bromine by PDMS, k_{Br} , is obtained by multiplying the bimolecular reaction constant between bromine and PDMS with the concentration of the reactants associated with PDMS, for example, $k_{Br} = k_{uw}w_o$. Values of k_{Br} for Model 3U are plotted as a function of mass in Figure 13D. The mean value is provided in Table 5. We note that the irreversible consumption rate k_{Br} is greater than the bulk rate constant α , shown in Figure 3. This is because reversible binding slows the mass transfer of bromine into PDMS, preventing the irreversible reaction from proceeding at the maximum rate.

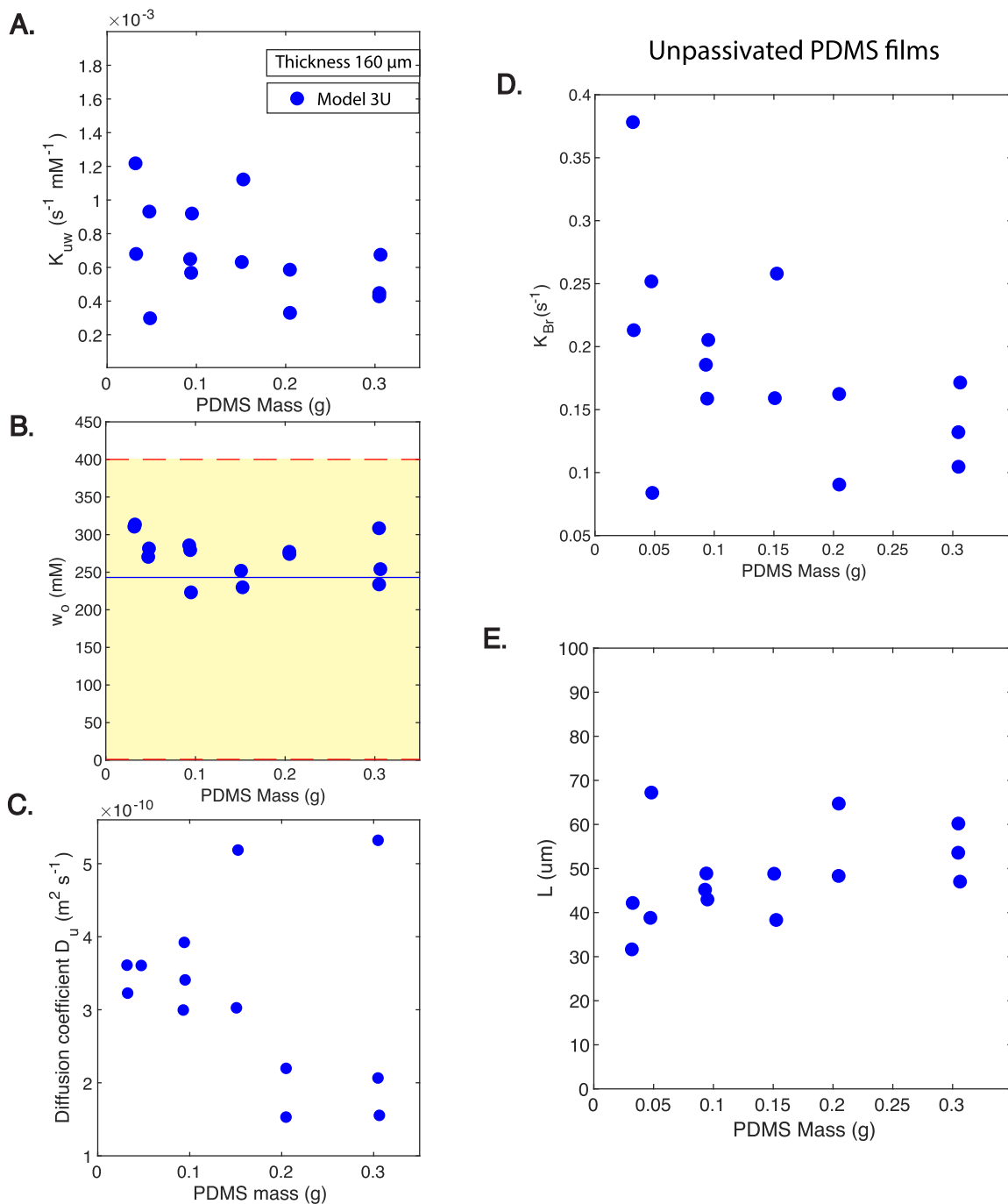


Figure 13. Fitted results from unpassivated PDMS films of $160 \mu\text{m}$ thickness as a function of mass. The absorbance data are shown in Figures 6 and 12. The average values of the fits are presented in Table 5. The symbols are the same for all panels: blue circles—Model 3U. (A) Bimolecular reaction constant, k_{uw} . (B) Concentration of the bromine reactants, w_o , in PDMS. The blue dashed line, $w_o = 244 \text{ mM}$, was used as an initial value for w_o in the fits, which were constrained to the range 0–400 mM (yellow shadowed region). (C) Diffusion coefficient, D_u . (D) Unimolecular bromine reaction rate, $k_{Br} = k_{uw}w_o$, obtained from multiplying data in (A,B) (see Table 5). (E) Reaction–diffusion length $L[\mu\text{m}] = \sqrt{D_u/k_{Br}}$ is calculated using the diffusion coefficients obtained in (C) and unimolecular bromine reaction rates in (D).

The reaction–diffusion length, $L = \sqrt{D_u/k_{Br}}$, measures the characteristic distance over which two sources of bromine can communicate through PDMS. The reaction–diffusion length is plotted as a function of mass in Figure 13E, and the average value for Model 3U is shown in Table 5. The reaction–diffusion length of the inhibitor bromine in PDMS is $L = 50 \mu\text{m}$.⁶ The reaction rate k_{Br} slows as the reactants w are

consumed; thus, the distance over which the points can couple through diffusion increases over time.

Fits: Unpassivated PDMS Films with the Same Mass and Different Thicknesses. We also examined unpassivated PDMS samples with a constant mass of 0.1 g for four different thicknesses, 160, 320, 480, and $720 \mu\text{m}$. Four data sets were collected with the thickness of $160 \mu\text{m}$ and two data sets per thickness for the other three thicknesses. We fit Model 3U to all data, holding some parameters fixed and allowing others to

Table 5. Summary of Fitting Results for Unpassivated PDMS Films of Thickness 160 μm ^a

coefficients	Model 3U
reaction constant k_{uw} ($10^{-4} \text{ s}^{-1} \text{ mM}^{-1}$)	6.77 ± 2.80
concentration of reactants w_o (mM)	270 ± 30
diffusion constant D ($10^{-9} \text{ m}^2/\text{s}$)	0.38 ± 0.25
bromine reaction rate k_{Br} (s^{-1})	0.18 ± 0.08
reaction-diffusion length L (μm)	50 ± 10

^aIndividual fits are shown in Figure 13. The absorbance data are shown in Figures 6 and 12.

vary, as indicated in Table 4. The absorbance as a function of time and the fittings with Model 3U (blue lines) are shown in Figure 7. The mean values of the fitting parameters obtained are presented in Table 6.

The fitted values of the diffusion constant vary by a factor of 4 for the four samples whose thickness varies by a factor of 4. This represents a systematic failure of Model 3U. However, it is notable that Model 3U performs much better than Model 1P for which the fitted diffusion constant varied by a factor of 10 for the fits to passivated films of the same dimensions as used here for unpassivated films. Further, we can use the values obtained from these fits to test our hypothesis that the experiments conducted for Model 2P were in the reaction-limited regime by calculating the Damköhler number. We obtain upper and lower bounds for Da by, respectively, plugging the slowest and fastest diffusion coefficients reported in Table 6 into eq 10. For the slower diffusion constant, Da was of the order 1–10 for all thicknesses; however, for the faster diffusion constant, Da was of the order of 0.1–1.0, which is in closer agreement with our original judgment that the experiments were dominated by reaction dynamics, for example, $Da < 1$. We therefore have more confidence in the faster diffusion coefficient, $D_u = 1.4 \times 10^{-9} \text{ m}^2/\text{s}$. We note that this value of the diffusion constant is very close to that reported for bromine in octane.¹⁶

CONCLUSIONS

First and foremost, the interaction of bromine and PDMS is complicated. Our experiments and models of bromine absorbance in the presence of PDMS suggest that bromine permeates into PDMS where it diffuses and reacts both reversibly and irreversibly with PDMS. This is the first time the latter two processes have been quantified. We have reached a number of conclusions, albeit with different degrees of certainty.

Table 6. Parameters, k_{uw} , D_u , and w_o , Obtained by Fitting Model 3U to the Absorbance Data Shown in Figure 7 for Unpassivated PDMS Films of Equal Mass (0.1 g) and Four Different Thicknesses (160, 320, 480, and 720 μm)^a

thickness	160 μm	320 μm	480 μm	720 μm
partition coefficient P_2^* (fixed)	12	12	12	12
off rate k_- (s^{-1}) (fixed)	0.0062	0.0062	0.0062	0.0062
reaction constant k_{uw} ($10^{-4} \text{ s}^{-1} \text{ mM}^{-1}$)	7.0 ± 1.5	4.2 ± 1.1	4.0 ± 0.42	9.3 ± 0.066
diffusion coefficient D_u ($10^{-9} \text{ m}^2/\text{s}$)	0.34 ± 0.037	0.67 ± 0.30	0.65 ± 0.070	1.4 ± 0.050
concentration of reactants w_o (mM)	260 ± 31	250 ± 20	290 ± 37	280 ± 14
bromine reaction rate k_{Br} (s^{-1})	0.18 ± 0.023	0.10 ± 0.019	0.11 ± 0.0026	0.26 ± 0.015
reaction-diffusion length L (μm)	44 ± 5	78 ± 11	76 ± 3	75 ± 1

^aThe partition coefficient and off rate (k_-) are fixed based on the results obtained from the fits to absorbance data from unpassivated PDMS films given in Table 2.

The parameters that result from the steady-state properties, the partition constant P and the concentration of bromine reactants within PDMS (w_o), are reliable. Our most firm quantitative result is that the partition coefficient of bromine between the PDMS elastomer and water is $P = [\text{Br}_2]_{\text{PDMS}}/[\text{Br}_2]_{\text{water}} = 12$. This is an equilibrium measurement and was robustly obtained from passivated samples. This result only relied on mass conservation, which is justified when the samples are carefully passivated. We also firmly established that bromine irreversibly reacts with PDMS and that PDMS only has a small concentration of bromine reactants, $w_o = 270 \pm 30$ mM. This measurement was also based on mass conservation and otherwise is model-independent. We note that the molar concentration of PDMS monomers in PDMS films is 100 times higher than w_o . The lack of stoichiometry between the bromine reactants and PDMS monomers suggests that bromine does not react with the PDMS monomer. Bromine could react with a partially linked cross-linker or with an unknown contaminant in commercial PDMS used in these experiments.

We immersed the PDMS films in concentrated bromine solutions and then observed the response of PDMS after removal. Initially, these bromine-passivated PDMS films were orange and opaque. They first underwent a rapid loss in the orange color associated with bromine diffusing out of the film, leaving the film white. This was followed by a slow loss of turbidity until they resembled the transparent films before exposure to bromine. The occurrence of different timescales for the loss of color and turbidity implies that the bromine-treated PDMS experienced two reversible processes, which led us to hypothesize that bromine both reversibly binds to and freely diffuses within PDMS.

We built minimal models to capture the transient response of bromine absorbance, which required us to identify four transport coefficients, k_+ , k_- , k_{uw} and D_u . We found these values to vary more across experiments than P and w_o . We noted that the absorbance measurements of passivated PDMS films of the same mass, but widely different thicknesses, had identical temporal responses upon exposure to bromine. This is incompatible with the free diffusion of bromine in PDMS being the dominant transport mechanism because the time for diffusive transport increases with the square of the film thickness. Instead, this indicates that bromine rapidly diffuses inside PDMS and slowly binds reversibly to PDMS. For these passivated films, we made the ansatz that they were in the reaction-limited regime, $Da \ll 1$, and thus were thin enough to be modeled as a homogeneous material. When we checked this assumption with the diffusion coefficients identified by subsequent experiments on unpassivated films, we found that

only the thickest films yielded a coefficient that satisfied this initial assumption. Additionally, as the dynamics of thicker samples will be more sensitive to the diffusion coefficient, we place more stock in these results. Still, our assumptions, along with the experimental limitations, lead to a systematic variation in the on and off rates k_{\pm} and the diffusion constant D_u as a function of film thickness. Our model and experiment therefore do not discriminate well between these processes and need improvement. Thus, we suggest that the reader exercise caution in accepting the values given for k_+ , k_- and D_u .

We measured the reaction rate of bromine with PDMS k_{uw} through analyzing absorbance experiments using unpassivated PDMS films. There was remarkably little variation in the fitted value for films of different mass and thickness.

Our experiments and modeling are based on bulk transport properties. However, there are a multitude of possible models incorporating free diffusion of bromine with the chemical kinetics of reversible and irreversible bond formation of bromine and PDMS. Without knowing the molecular identity of the reactants and the precise chemical kinetics, our models yield fits to transport parameters that are little more than educated guesses. To proceed further, it will be necessary to identify molecular mechanisms for the interaction between bromine and PDMS.

The principal motivation for our studies was to establish the degree to which PDMS is a suitable substrate for the engineering of reaction–diffusion networks of BZ chemical oscillators that are coupled by the diffusive flux of bromine. This work provides the material constants and theoretical framework necessary to quantitatively model the coupling strength of coupled BZ oscillators. Specifically, we recommend using the parameters given in Table 6 for the films of thicknesses 480 and 720 μm in any model constructed to treat the transport of bromine through PDMS. This work also establishes that PDMS has the potential to be an excellent material for the manufacture of BZ reaction–diffusion networks, albeit with the following caveats. On the one hand, the concentration of the bromine reactants, w_o , is low, implying that PDMS networks could first be fabricated and then passivated to eliminate the undesirable irreversible reaction between bromine and PDMS. On the other hand, thin films of PDMS are delicate, so manufacturing thin passivated PDMS films suitable for studying the dynamics of BZ chemical networks could prove challenging. For unpassivated films, the oscillators should be separated by less than the reaction–diffusion length, $L = \sqrt{D_u/k_{\text{Br}}} \sim 50 \mu\text{m}$, and for both passivated and unpassivated films, the amount of PDMS in contact with the oscillators should be minimized.

MATERIALS

Bromine (Br_2) was supplied by Sigma-Aldrich in liquid form.

Sodium thiosulfate anhydrous was supplied by Sigma-Aldrich and was used as a neutralizing solution for safety precaution and disposal of bromine water and PDMS (see Supporting Information).

The elastomer silicone (PDMS) was Sylgard 184 (Dow Corning, Sylgard 184 Silicone Encapsulant Clear, 0.5 kg Kit). The base and cross-linker agents were used with the ratio of 10:1 (w/w) and mixed using the centrifugal mixer Thinky planetary nonvacuum centrifugal mixer AR-250.

The stainless steel wafers used for the spin-coating of PDMS for the creation of PDMS layers had a diameter of 7.62 cm and a

thickness of 0.074 cm (product number: 304 Stainless Steel Sheet #8 Mirror (22G (0.0293"))), and they were supplied by Stainless supply, a JW Metal Products company (<https://www.stainlesssupply.com>).

Absorbance Spectroscopy Data. The absorbance data were collected with a Vernier Ocean optics spectrometer V-SPEC and recorded with the software program Logger-Pro. The raw data were filtered with the use of Minitab and normalized and averaged with MATLAB.

Optical Cuvettes. The spectrometer cells were 10 mm square Quartz cuvettes, with 3.5 mL volume with glass stoppers (Starna cells).

Computational Fitting Models. All reaction–diffusion models used in fitting were numerically integrated in MATLAB using the method of lines. In this technique, spatial derivatives were discretized to create a coupled system of nonlinear differential equations that were then solved using ODE45. The fitting of the models (eqs 4–9) to the data was done using least-square minimization.

ASSOCIATED CONTENT

SI Supporting Information

The Supporting Information is available free of charge at <https://pubs.acs.org/doi/10.1021/acs.jpcb.1c01552>.

Spinning programs for thin PDMS films with different thicknesses; absorption spectrum of brominated water as a function of bromine concentration; passivated PDMS thin-film data; qualitative evaluation of the PDMS transparency change; estimation of the PDMS reactant concentration; absorbance of passivated and unpassivated PDMS films; effective diffusivity of Model 3U; and analytical solution of Model 2P ([PDF](#))

Video showing the color change of thin PDMS films right after passivation with bromine ([AVI](#))

Video showing the transparency change of thin PDMS films starting 10 min after passivation with bromine ([AVI](#))

AUTHOR INFORMATION

Corresponding Author

Seth Fraden – Department of Physics, Brandeis University, Waltham, Massachusetts 02453, United States; Phone: 781-736-2888; Email: fraden@brandeis.edu

Authors

Maria Eleni Moustaka – Department of Physics, Brandeis University, Waltham, Massachusetts 02453, United States;  orcid.org/0000-0003-4479-1775

Michael M. Norton – Department of Physics, Brandeis University, Waltham, Massachusetts 02453, United States

Baptiste Blanc – Department of Physics, Brandeis University, Waltham, Massachusetts 02453, United States

Viktor Horvath – Department of Physics, Brandeis University, Waltham, Massachusetts 02453, United States

S. Ali Aghvami – Department of Physics, Brandeis University, Waltham, Massachusetts 02453, United States

Complete contact information is available at: <https://pubs.acs.org/10.1021/acs.jpcb.1c01552>

Notes

The authors declare no competing financial interest.

ACKNOWLEDGMENTS

M.E.M., B.B., V.H., M.M.N., and S.F. devised the experiments. M.E.M. fabricated the PDMS films and built the z-micrometer controlled stage. M.M.N. developed the computational fitting models. M.E.M. performed and analyzed the experiments. A.A. acquired the images of the time lapse of passivated PDMS cubes. S.F., M.M.N., and M.E.M. developed the figures and wrote the manuscript. M.M.N., B.B., and V.H. are acknowledged as second coauthors. The authors would like to acknowledge funding from NSF DMREF-1534890, the U.S. Army Research Laboratory, and the U.S. Army Research Office under contract/grant no. W911NF-16-1-0094, and the funding of the microfluidics facility at Brandeis through NSF MRSEC DMR-2011486.

REFERENCES

(1) Toepke, M. W.; Beebe, D. J. PDMS absorption of small molecules and consequences in microfluidic applications. *Lab Chip* **2006**, *6*, 1484–1486.

(2) Mukhopadhyay, R. When PDMS isn't the best. *Anal. Chem.* **2007**, *79*, 3248–3253.

(3) Wang, J. D.; Douville, N. J.; Takayama, S.; ElSayed, M. Quantitative analysis of molecular absorption into PDMS microfluidic channels. *Ann. Biomed. Eng.* **2012**, *40*, 1862–1873.

(4) Shim, J.-U.; Cristobal, G.; Link, D. R.; Thorsen, T.; Fraden, S. Using Microfluidics to Decouple Nucleation and Growth of Protein Crystals. *Cryst. Growth Des.* **2007**, *7*, 2192–2194.

(5) Tompkins, N.; Cambria, M. C.; Wang, A. L.; Heymann, M.; Fraden, S. Creation and perturbation of planar networks of chemical oscillators. *Chaos* **2015**, *25*, 064611.

(6) Litschel, T.; Norton, M. M.; Tserunyan, V.; Fraden, S. Engineering reaction–diffusion networks with properties of neural tissue. *Lab Chip* **2018**, *18*, 714–722.

(7) Sheehy, J.; Hunter, I.; Moustaka, M. E.; Aghvami, S. A.; Fahmy, Y.; Fraden, S. Impact of PDMS-Based Microfluidics on Belousov–Zhabotinsky Chemical Oscillators. *J. Phys. Chem. B* **2020**, *124*, 11690–11698.

(8) Field, R. J.; Körös, E.; Noyes, R. M. Oscillations in chemical systems. II. thorough analysis of temporal oscillation in the bromate-cerium-malonic acid system. *J. Am. Chem. Soc.* **1972**, *94*, 8649–8664.

(9) Noyes, R. M.; Field, R.; Körös, E. Oscillations in chemical systems. I. detailed mechanism in a system showing temporal oscillations. *J. Am. Chem. Soc.* **1972**, *94*, 1394–1395.

(10) Vanag, V. K.; Epstein, I. R. A model for jumping and bubble waves in the Belousov–Zhabotinsky–aerosol OT system. *J. Chem. Phys.* **2009**, *131*, 104512.

(11) Tompkins, N.; Li, N.; Girabawe, C.; Heymann, M.; Ermentrout, G. B.; Epstein, I. R.; Fraden, S. Testing Turing's theory of morphogenesis in chemical cells. *Proc. Natl. Acad. Sci. U.S.A.* **2014**, *111*, 4397–4402.

(12) Norton, M. M.; Tompkins, N.; Blanc, B.; Cambria, M. C.; Held, J.; Fraden, S. Dynamics of Reaction-Diffusion Oscillators in Star and other Networks with Cyclic Symmetries Exhibiting Multiple Clusters. *Phys. Rev. Lett.* **2019**, *123*, 148301.

(13) Buskohl, P. R.; Vaia, R. A. Belousov–Zhabotinsky autonomic hydrogel composites: Regulating waves via asymmetry. *Sci. Adv.* **2016**, *2*, No. E1600813.

(14) King, P. H.; Corsi, J. C.; Pan, B.-H.; Morgan, H.; de Planque, M. R. R.; Zauner, K.-P. Towards molecular computing: Co-development of microfluidic devices and chemical reaction media. *BioSystems* **2012**, *109*, 18–23.

(15) Ginn, B. T.; Steinbock, B.; Kahveci, M.; Steinbock, O. Microfluidic systems for the Belousov–Zhabotinsky reaction. *J. Phys. Chem. A* **2004**, *108*, 1325–1332.

(16) Rossi, F.; Vanag, V. K.; Tiezzi, E.; Epstein, I. R. Quaternary Cross-Diffusion in Water-in-Oil Microemulsions Loaded with a Component of the Belousov–Zhabotinsky Reaction. *J. Phys. Chem. B* **2010**, *114*, 8140–8146.

(17) Toiya, M.; Vanag, V. K.; Epstein, I. R. Diffusively Coupled Chemical Oscillators in a Microfluidic Assembly. *Angew. Chem., Int. Ed.* **2008**, *47*, 7753–7755.

(18) Van Meer, B. J.; de Vries, H.; Firth, K. S. A.; van Weerd, J.; Tertoolen, L. G. J.; Karperien, H. B. J.; Jonkheijm, P.; Denning, C.; Ijzerman, A. P.; Mummery, C. L. Small molecule absorption by PDMS in the context of drug response bioassays. *Biochem. Biophys. Res. Commun.* **2017**, *482*, 323–328.

(19) Auner, A. W.; Tasneem, K. M.; Markov, D. A.; McCawley, L. J.; Hutson, M. S. Chemical-PDMS binding kinetics and implications for bioavailability in microfluidic devices. *Lab Chip* **2019**, *19*, 864–874.

(20) O'Neil, M. e. *The Merck Index: An Encyclopedia of Chemicals, Drugs, and Biologicals*; The Royal Society of Chemistry, 2013; p 246.

(21) Goldschleger, I. U.; Senekerimyan, V.; Krage, M. S.; Seferyan, H.; Janda, K. C.; Apkarian, V. A. Quenched by ice: Transient grating measurements of vibronic dynamics in bromine-doped ice. *J. Chem. Phys.* **2006**, *124*, 204507.

(22) Gutmann, H.; Lewin, M.; Perlmuter-Hayman, B. Ultraviolet absorption spectra of chlorine, bromine, and bromine chloride in aqueous solution. *J. Phys. Chem.* **1968**, *72*, 3671–3673.

(23) Bayliss, N.; Cole, A.; Green, B. The Visible Absorption Spectrum of Bromine in Solution. *Aust. J. Chem.* **1948**, *1*, 472–479.

(24) Cavallo, G.; Metrangolo, P.; Milani, R.; Pilati, T.; Priimagi, A.; Resnati, G.; Terraneo, G. The Halogen Bond. *Chem. Rev.* **2016**, *116*, 2478–2601.

(25) Hong, H. C.; Chen, C. M.; Chou, Y. C.; Lin, C. H. Study of novel electrical routing and integrated packaging on bio-compatible flexible substrates. *Microsyst. Technol.* **2010**, *16*, 423–430.

(26) Lee, J. N.; Park, C.; Whitesides, G. M. Solvent Compatibility of Poly(dimethylsiloxane)-Based Microfluidic Devices. *Anal. Chem.* **2003**, *75*, 6544–6554.

(27) Hourlier-Fargette, A.; Dervaux, J.; Antkowiak, A.; Neukirch, S. Extraction of Silicone Uncrosslinked Chains at Air–Water–Polydimethylsiloxane Triple Lines. *Langmuir* **2018**, *34*, 12244–12250.

(28) Hong, T.; Niu, Z.; Hu, X.; Gmernicki, K.; Cheng, S.; Fan, F.; Johnson, J. C.; Hong, E.; Mahurin, S.; Jiang, D.-E.; et al. Effect of cross-link density on carbon dioxide separation in polydimethylsiloxane-norbornene membranes. *ChemSusChem* **2015**, *8*, 3595–3604.